Nonlinear vs. Linear Mesoscale Dynamics

G. Leoncini and R. A. Pielke Sr.

Dept of Atmospheric Science, Colorado State University, Fort Collins CO

Presented at Adelphi, MD, Annual CG/AR Program Review, November 14, 2005

Introduction

Regular Numerical Weather Prediction models aim to provide accurate forecasts for any weather pattern, topography, and landuse, therefore they require the numerical integration of the full motion and heat equations, and several parameterizations which notoriously increase the computational costs limiting the ability to produce reliable fine spatial-scale real-time or near real-time weather forecasts. This problem can be partially overcome with the use of specialized models. For example if a particular situation, or weather pattern for a specific location, is known to be well approximated by a linear model then it is possible to use an analytical solution which has the advantage of being exact and runs considerably faster. Another possibility, with similar advantages, is to use an analytical solution for the linear component and integrate numerically only the nonlinear one. This approach already proved successful for the shallow water equation (Weidman and Pielke, 1983). A third possible application consists in knowing whether the atmosphere is prevalently hydrostatic, because in this case pressure and temperature profiles can easily and quickly be obtained from each other, increasing the importance of remote sensing observations of one or the other variable. In other words, the knowledge of these important characteristics of the atmosphere allows to design specialized models which simulate the weather in a accurate and time efficient fashion, since they would solve only the relevant part of the equations. With these applications in mind, Leoncini and Pielke (2005) investigate the relevance of several terms in the equations which simulate mesoscale dry flow equations over a wide range of temporal and spatial scales within the framework of Dalu et al. (2003). Specifically, a modified version of the Regional Atmospheric Modeling System was used to compute the individual terms of advection, Coriolis effect, buoyancy, and dynamical pressure, as they appear in the Laplacian of the geopotential, for the cases of linearized advection and fully nonlinear advection. In both cases, the atmosphere was forced with the same sensible heat fluxes. More specifically, Leoncini and Pielke (2005) found that the change in the Laplacian of the geopotential from linearized to full advection are due to the change in vertical gradient of buoyancy (b_z) and in the "residual" which depends upon the vertical derivatives of the background potential temperature, while Dalu et al. found that the main factors are the nonlinear advection of mass and the nonlinear advection of buoyancy. The main goal of this study is to address this discrepancy.

DoD Relevance

The overall aim of this research is to determine which approximations can be made to the dynamical core of a mesoscale model without losing accuracy in the forecast, with forcings that span several scales in time and space. Once this research is completed models specific to those scales can be built. Their will be the reduced computational cost without loss of accuracy.

The Equations

In order to better explain these differences, and to validate and extend the conclusion of Dalu et al., we modified RAMS such that it integrates the same equations as in Dalu et al., with the ability to turn on terms which correspond to more general assumption. More specifically, assuming $\theta=\theta_0+\theta(\mathbf{z})+\theta'(\mathbf{x},\mathbf{z},\mathbf{t})$, and $\pi=\pi_0(\mathbf{z})+\pi'(\mathbf{x},\mathbf{z},\mathbf{t})$ where θ is the potential temperature and π the Exner function, the first important modification we made to RAMS is the large scale background state: it is usually assumed to be $(\theta_0+\theta(\mathbf{z}))\partial_{\mathbf{z}}\pi_0=-\mathbf{g}$, but we adopted Dalu et al: $\theta_0\partial_{\mathbf{z}}\pi_0=-\mathbf{g}$. Dalu et al. also chose to define geopotential as $\phi=\theta_0\pi'$, while RAMS uses π' only. As per the u and v-momentum equations, we also added the Rayleigh coefficient (λ in Table 1), and represented turbulence with a constant eddy coefficient K. U is set to a constant value for the linearized advection case, and to u for the full advection one. With these modifications and definitions, the u and v-momentum equations are identical (see Table 1). The third column of Table 1 shows two additional terms which have been dropped from the right hand side during the Reynolds averaging in Dalu et al., but that will be retained when extending the theory. Defining buoyancy b as $\mathbf{b}=\mathbf{g}\,\theta'/\theta_0$, again Table 1 shows that also the w-momentum equation in our version of RAMS is essentially identical to Dalu et al. For this equation also two terms neglected in Dalu et al. can be retained. RAMS θ equation is shown in Table 1, and with all the above definitions and modifications, and allowing only the vertical advection of the background potential temperature also this one is identical to Dalu et al. ***b*** equation if multiplied by $\mathbf{g}/\theta_0$, with $\mathbf{N}^2=\frac{\mathbf{g}}{\theta_0}\frac{\partial\theta(\mathbf{z})}{\partial\mathbf{z}}$. RAMS continuity equation has not been modified since compressibility should be negligible (Klemp and Wilhelmson 1978) and keeping track of the Exner function tendency allows to verify this assumption.

	Equation	Additional Terms
u-mom Dalu et al	$\left(\frac{\partial}{\partial \mathbf{t}}+\lambda\right)\mathbf{u}+\mathbf{U}\frac{\partial \mathbf{u}}{\partial \mathbf{x}}-\mathbf{fv}+\frac{\partial\phi}{\partial \mathbf{x}}=\mathbf{K}\left(\frac{\partial^2}{\partial \mathbf{x}^2}+\frac{\partial^2}{\partial \mathbf{z}^2}\right)\mathbf{u}$	
u-mon RAMS	$\left(\frac{\partial}{\partial \mathbf{t}}+\lambda\right)\mathbf{u}+\mathbf{U}\frac{\partial \mathbf{u}}{\partial \mathbf{x}}-\mathbf{fv}+\vartheta_0\frac{\partial\pi'}{\partial \mathbf{x}}=\mathbf{K}\left(\frac{\partial^2}{\partial \mathbf{x}^2}+\frac{\partial^2}{\partial \mathbf{z}^2}\right)\mathbf{u}$	$-\left(\vartheta(\mathbf{z})+\vartheta'\right)\frac{\partial\pi'}{\partial \mathbf{x}}$
w-mom Dalu et al	$\left(\frac{\partial}{\partial \mathbf{t}}+\lambda\right)\mathbf{w}+\mathbf{U}\frac{\partial \mathbf{w}}{\partial \mathbf{x}}+\frac{\partial\phi}{\partial \mathbf{z}}-\mathbf{b}=\mathbf{K}\left(\frac{\partial^2}{\partial \mathbf{x}^2}+\frac{\partial^2}{\partial \mathbf{z}^2}\right)\mathbf{w}$	
w-mom RAMS	$\left(\frac{\partial}{\partial \mathbf{t}}+\lambda\right)\mathbf{w}+\mathbf{U}\frac{\partial \mathbf{w}}{\partial \mathbf{x}}+\theta_0\frac{\partial\pi'}{\partial \mathbf{z}}-\mathbf{g}\frac{\theta'}{\theta_0}=\mathbf{K}\left(\frac{\partial^2}{\partial \mathbf{x}^2}+\frac{\partial^2}{\partial \mathbf{z}^2}\right)\mathbf{w}$	$-\vartheta'\frac{\partial\pi'}{\partial \mathbf{z}}+\vartheta(\mathbf{z})\frac{\partial\pi}{\partial \mathbf{z}}$
b Dalu et al	$\left(\frac{\partial}{\partial \mathbf{t}}+\lambda\right)\mathbf{b}+\mathbf{u}\frac{\partial \mathbf{b}}{\partial \mathbf{x}}+\mathbf{N}^2\mathbf{w}=\mathbf{Q}+\mathbf{K}\left(\frac{\partial^2}{\partial \mathbf{x}^2}+\frac{\partial^2}{\partial \mathbf{z}^2}\right)\mathbf{b}$	
θ *RAMS*	$\left(\left(\frac{\partial}{\partial \mathbf{t}}+\lambda\right)\theta+\mathbf{u}\frac{\partial\theta}{\partial \mathbf{x}}+\mathbf{w}\frac{\partial\theta(\mathbf{z})}{\partial \mathbf{z}}=\mathbf{F}+\mathbf{K}\left(\frac{\partial^2}{\partial \mathbf{x}^2}+\frac{\partial^2}{\partial \mathbf{z}^2}\right)\theta\right)\frac{\mathbf{g}}{\theta_0}$	$-\mathbf{w}\frac{\partial\theta'}{\partial \mathbf{z}}\frac{\mathbf{g}}{\theta_0}$
Continuity Dalu et al	$\frac{\partial \mathbf{u}}{\partial \mathbf{x}}+\frac{\partial \mathbf{w}}{\partial \mathbf{z}}=0$	
Continuity RAMS	$\frac{\partial\pi'}{\partial \mathbf{t}}=-\frac{\mathbf{R}\pi_0}{\mathbf{C}_v\rho_0\theta_0}\left(\frac{\partial\rho_0\theta_0\mathbf{u}}{\partial \mathbf{x}}+\frac{\partial\rho_0\theta_0\mathbf{w}}{\partial \mathbf{z}}\right)$	

Table 1 Dalu et al. (2003) mesoscale equations compared against our modified version of RAMS

Methodology

In order to retain as many similarities as possible with Dalu et al. (2003), we held the Coriolis term constant, and ran 2D simulations. We also set the eddy viscosity coefficient ***K***, equal to 0 to simplify the analytical solution and to avoid boundary condition related issues, RAMS was forced only by a periodic (in time and space) heat flux divergence exponentially decreasing with height of the form:

$$\mathbf{Q}=\mathbf{Q}_0\exp\left(\frac{-\mathbf{z}}{\mathbf{L}_z}\right)\cos\left(\frac{2\pi}{\mathbf{T}}\mathbf{t}+\frac{2\pi}{\mathbf{L}_x}\mathbf{x}\right)$$

Q_0 and L_z were both held constant for every simulation, respective values are 5.78703 10-5 Ks^{-1} (or 5 K day^{-1}), and 1000 m. The initial pressure profile was originally chosen for the regular hydrostatic background state, and therefore the model was run for 30 min without any forcing to reach a balanced state with negligible vertical velocities. An important environmental parameter is the lapse rate which was 3 Kkm^{-1}, up to 1 km, and increasingly stable up to the tropopause. The vertical grid spacing was the same across all the simulations and had an initial Δz of 25 m, with a stretching of 1.12. The horizontal wavelength L_x was 10 km. Initial tests demonstrated a significant sensitivity to resolution and grid spacing of one fortieth of the wavelength was chosen, so that simulations would have a good numerical representation of the wave with no significant damping or phase shift. Domain encompassed two full wavelengths. Every simulation was carried out for the spin up time and one hour correspondent to the wave period. The background winds were always westerly of either 0 or 2.5 m s^{-1}. Every configuration was also run with the full and with linear advection (FA, LA) as described in the introduction. During the simulations all the terms of the Poisson equations for ϕ are diagnosed, according to:

$$\nabla^2\phi=-\nabla\cdot\left(\mathbf{T}\vec{\mathbf{u}}\right)+\mathbf{f}\mathbf{v}_x+\mathbf{b}_z$$

which corresponds to Dalu et al. Eq. 32, and where T is the operator that accounts for the time derivative, the Rayleigh friction, and the advection. Subscripts indicate derivatives. The first term represent the dynamic pressure and the third is the vertical derivative of buoyancy, in which is embedded the time evolution of the convergence of buoyancy advection. The above mentioned terms are responsible for the changes in the geopotential, according to Dalu et al. Also the differences FA-LA are also evaluated, to at least estimate the different contribution to the nonlinear geopotential.

Results

The temperature perturbation at the end of the period for the nonlinear case with 0 m s^{-1} background wind is shown in Fig. 1. The cooling-warming pattern is slanted because the forcing travels westward (to the right) and the resulting flow has a vertically oscillating component (Dalu et al. 2003). The different slope of the pattern above 1000 m, that is above the boundary layer is due to the increased vertical stability. The other three simulations result in similar patterns.

All the simulations show that the Coriolis term of the Laplacian changes very little from the linear to the nonlinear case and the nonlinear convergence of mass dominates the changes in the Laplacian of the geopotential (Fig. 2-4) .

Conclusions and Future Work

In agreement with Dalu et al. (2003), the nonlinear convergence of mass is responsible for the changes in the Laplacian of the geopotential over most of the atmosphere, at least in cases presented here, that is a forcing period of 1 h, wavelength of 10 km, and a large scale background wind of 0 and 2.5 ms^{-1}. In the immediate future, we plan to extend this analysis to a wider range of scales, in space and time. Specifically, we plan to more carefully evaluate the significance of the buoyancy advection by running simulations with no Rayleigh friction and zero background wind, that is when the evaluation does not involve integral equations, and for which we can easily compute an analytical solution, that will provide further solidity to the model. Lastly we will evaluate the terms of the equations that have been neglected in order to extend the theory to a more realistic atmosphere. In the longer term specialized independent models will be built and comparisons against regular NWP mesoscale models will be carried out.

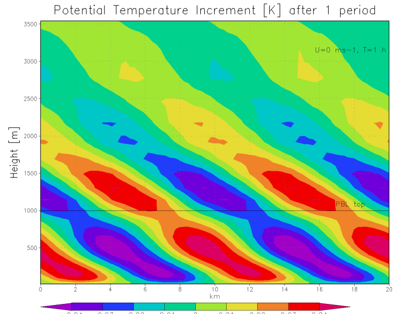

Fig. 1 Potential temperature increment after one period the nonlinear case, with L_x = 10 km, T= 1h, u_0=0 m s^{-1}.

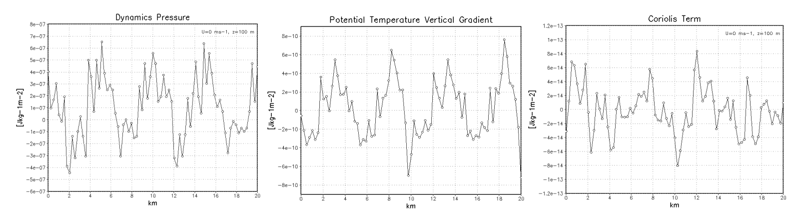

Fig. 2 Contributions to the geopotential difference between the nonlinear and linear cases for L_x = 10 km, T= 1h, u_0=2.5 m s^{-1} at z = 12 m.

corresponding author address: Giovanni Leoncini Dept of Atmospheric Science, Colorado State University, Ft Collins, CO 80523.
E-mail: leoncini@atmos.colostate.edu

References

Dalu, G.A., M. Baldi, R.A. Pielke Sr., and G. Leoncini, 2003: Mesoscale nonhydrostatic and hydrostatic pressure gradient forces: Theory and parameterization. ***J. Atmos. Sci.***, **60**, 2249-2266.

Leoncini, G., and R.A. Pielke Sr., 2005: Nonlinear vs. linear dynamics. Poster Presentation, Battlespace Atmospheric and Cloud Impacts on Military Operations (BACIMO) 2005 Conference, Monterey, California, October 12-14, 2005. Available at http://blue.atmos.colostate.edu/presentations/PPT-43.pdf

Rotunno,R.,1983: On the linear theory of land and seabreeze. ***J. Atmos.Sci.***,**40**,1999–2009.

Weidman, S.T. and R.A. Pielke, 1983: A more accurate method for the numerical solution of nonlinear partial differential equations. ***J. Comput. Phys.***, **49**, 342-348.

Acknowledgment: This research is supported by the DoD Center for Geoscience/Atmospheric Research at Colorado State University under cooperative agreement DAAD19-02-2-0005 with the Army Research Laboratory.